The effect of doping Ag on the microstructure of $La_{2/3}Sr_{1/3}MnO_3$ films

Q. Zhan, R. Yu, L.L. He, and D.X. Li
Shenyang National Laboratory for Materials Science, Institute of Metal Research, Chinese Academy of Sciences, 72 Wenhua Road, Shenyang 110016, Peoples' Republic of China

J. Li and C.K. Ong
Center for Superconducting and Magnetic Materials and Department of Physics, National University of Singapore, Singapore 119260

(Received 2 July 2002; accepted 30 July 2002)

The microstructure of Ag-doped $La_{2/3}Sr_{1/3}MnO_3$ (LSMO) thin films deposited on (001) $LaAlO_3$ single-crystal substrates was systematically investigated in cross section and plan view by high-resolution electron microscopy and analytical electron microscopy. The results showed that the films deposited at 750 °C were perfectly epitaxial with or without Ag-doping. No Ag in the doped film was detected. On the other hand, the LSMO films deposited at 400 °C were less perfect. With increasing Ag-doping level, the shape of LSMO grains became irregular, and the grain size increased gradually. Large polycrystalline clusters consisting of LSMO, AgO, and Ag grains formed in the doped films, and the amount and size of them increased with increasing Ag-doping level. Ag existed at the LSMO grain boundaries in its elemental state. A growth process for the LSMO-Ag system is discussed based on the experimental results. The enhancement of the magnetic spin disorders at the grain boundaries and interfaces caused by doping Ag could result in an improvement of low-field magnetoresistance.

I. INTRODUCTION

Mixed valence manganites with perovskite structure exhibit two kinds of magnetoresistance (MR): intrinsic or intragrain MR observed in the vicinity of magnetic transition temperature T_c and extrinsic or intergrain MR occurring over a wide temperature range below T_c.[1,2]

The well-known colossal magnetoresistance (CMR), explained by the double exchange interactions,[3] is an intrinsic effect. However, the sharp drop in resistance was achieved only in a high magnetic field in the Tesla range, thus severely limiting the potential applications of CMR materials. On the contrary, the intergrain magnetoresistance usually obtained in an applied field of a few hundred Oersted has attracted special interest.[4–7] In particular, polycrystalline samples have shown the significant low-field effect, which becomes increasingly important at low temperatures. It was shown that low-field MR is dominated by the grain boundaries.[5,6] Spin-polarized tunneling[4] or spin-dependent scattering[6] through or at the grain boundaries is believed to be responsible for it. Researchers explore various methods for enhancing the low-field MR as highly as possible, such as polycrystalline bulk,[4,8] polycrystalline thin films,[5,9] artificially induced grain boundaries,[10] and trilayer tunnel junctions.[11] It seems that introducing weak-link grain boundaries and interfaces is a promising way to enhance the low-field MR value in manganite films.[12] Since the physical properties, in particular the MR effect, are sensitive to the structure of perovskite-related manganites, it is expected that the extrinsic MR would be enhanced by doping to modify the microstructure of materials.

Ag has been widely used as the most suitable dopant to improve superconducting properties in materials such as $YBa_2Cu_3O_{7-\delta}$ (YBCO).[13–17] It is well known that the addition of Ag to YBCO leads to an increase in the critical current density, which is believed to be caused by a "catalytic" effect of Ag dispersed at grain boundaries. Evidence for this was obtained through scanning electron microscopy (SEM).[16] Studies on the addition of Ag to perovskite manganites, including thin films and bulk polycrystalline samples, were also reported recently by a few groups.[18–20] They found improvement in several desirable properties, such as the higher ferromagnetic transition and the metal–insulator transition temperatures or large MR value at room temperature. However, the microstructural effects have not been analyzed clearly. In particular, the existent stage and position of Ag-dopant are always argued due to lack of detailed microstructural studies.

In this work, the changes of microstructure in $La_{2/3}Sr_{1/3}MnO_3$ (LSMO) thin films with different Ag-doping level were investigated systematically by high-resolution electron microscopy (HREM) and analytical electron microscopy (AEM) in cross-section and plan-view. Direct evidence for the effect of doping Ag on the microstructure of LSMO films was provided. A growth process for the LSMO-Ag system is also discussed. These results could be helpful in understanding the microscopic transport mechanisms and therefore the extrinsic MR effect.

II. EXPERIMENTAL

The ceramic target LSMO was sintered by conventional solid-state reaction. A metal Ag target was adopted for doping. Co-deposition of LSMO and Ag on (001) $LaAlO_3$ (LAO) single-crystal substrates was performed by a dual-beam pulsed laser ablation (PLA) system.[21] The laser frequency on the LSMO target was kept at 4 Hz while that on the Ag target (Ag repeat rate) was adjusted from 0 to 6 Hz using a chopper. Substrate temperatures of 750 and 400 °C were chosen for comparison. The films were kept *in situ* for 1 h before they were cooled down slowly. An oxygen pressure of 0.2 mbar was adopted during the deposition and subsequent annealing procedure.

Samples with different doping levels of Ag are defined as HT*n*/4 and LT*n*/4, where HT and LT denote substrate temperatures of 750 °C and 400 °C, respectively; 4 and *n* denote the laser repeat rate for LSMO and Ag targets, respectively. For example, HT0/4 represents a stoichiometric LSMO film deposited at 750 °C; while LT6/4 denotes a co-deposited film deposited at 400 °C with Ag repeat rate of 6 Hz.

The cross section as well as plan view samples suitable for transmission electron microscopy (TEM) and HREM studies were prepared by standard techniques described previously in detail.[22] The microstructures of LSMO films with different Ag-doping levels were characterized by a JEM 2010 HREM (JEOL Ltd., Tokyo, Japan) with a point-to-point resolution of 0.19 nm. Composition analysis was carried out using a HF 2000 cold field-emission-gun TEM (Hitachi Ltd., Tokyo, Japan) equipped with an Oxford Link ISIS energy dispersive spectroscopy (EDS) system (Oxford Instruments, Buckinghamshire, U.K.).

III. RESULTS

A. Films deposited at T_s = 750 °C

Figure 1 shows the cross-sectional morphologies of the LSMO films deposited at 750 °C with laser frequencies on the Ag target of 0 Hz (HT0/4) and 4 Hz (HT4/4), respectively. The insets are corresponding selected-area electron diffraction (SAED) patterns. The direction of incident electron beam was along $[100]_c$ of the substrate (for simplicity, the indexing was referred to the pseudo-cubic structure), parallel to the interface. Both of the films exhibit uniform thickness and flat interfaces.

Figure 2 illustrates typical plan-view morphologies of the films and corresponding electron diffraction patterns (EDPs) along $[001]_c$ zone axis. The cross-sectional and plan-view single-crystal EDPs indicate that the films are not only epitaxial well along the *c* axis (film-normal) but also in the *ab* plane for different doping levels of Ag. The undoped film, HT0/4, consists of rectangularlike shaped grains, about 50 nm in size [Fig. 2(a)]. This mosaiclike grain alignment suggests that the film is formed by the coalescence of epitaxial islands.[23] Distinct bright contrasts among the LSMO grains where the coalescence of epitaxial islands meet were left. The HREM image of the intergranular region is shown in Fig. 3. The plan-view image of HT4/4 predominantly exhibits moiré fringes and arrays of misfit dislocations. Figure 2(b) shows a square network of misfit dislocations caused

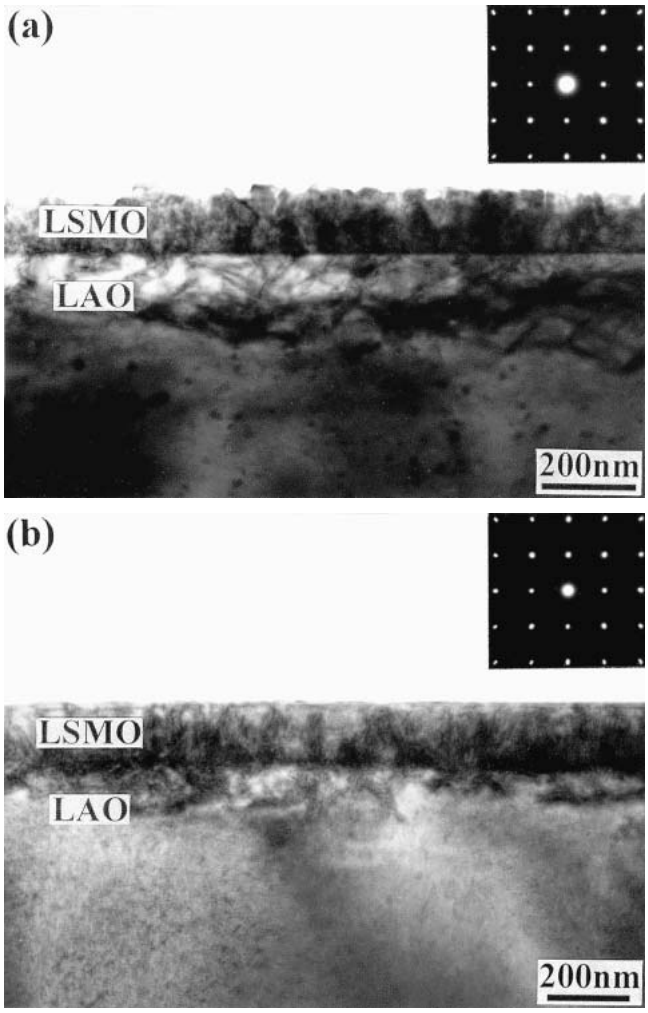

FIG. 1. Cross-sectional morphologies of the (a) undoped HT0/4 and (b) Ag-doped HT4/4 LSMO films deposited at 750 °C. The insets are corresponding EDPs, both showing perfect epitaxy along *c* axis.

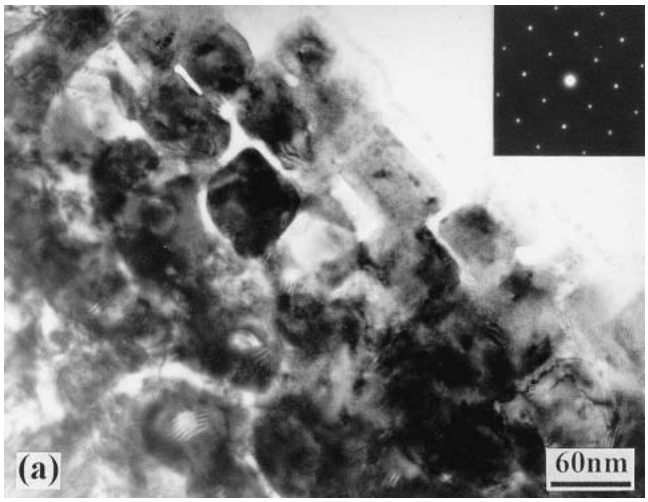

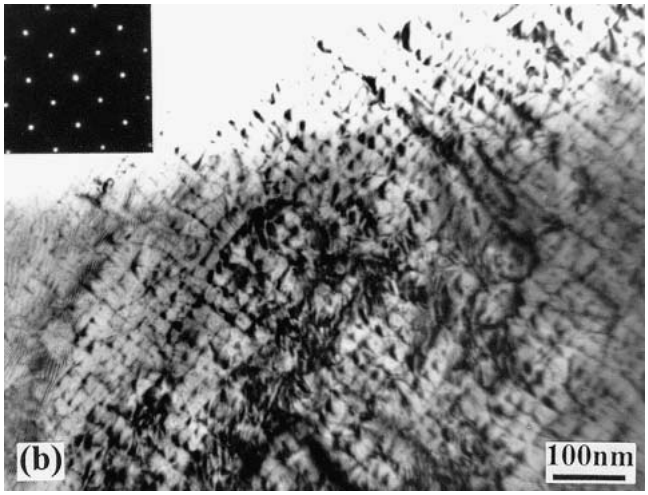

FIG. 2. Plan-view morphologies of (a) HT0/4 and (b) HT4/4 deposited at 750 °C. The insets are corresponding EDPs.

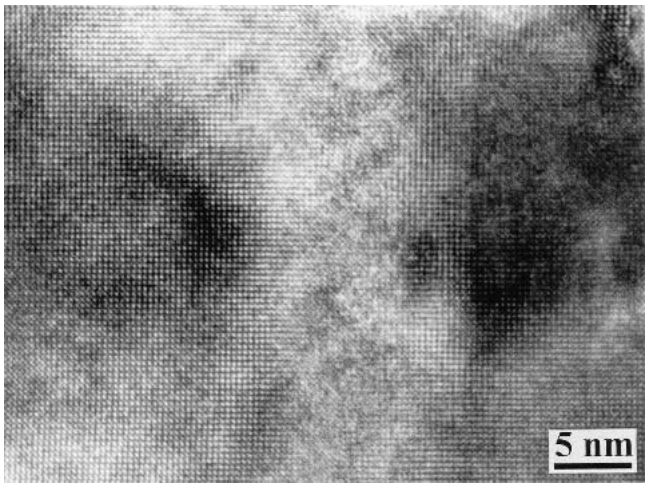

FIG. 3. HREM image of the intergranular region between LSMO grains in HT0/4.

by the lattice mismatch between the LSMO film and the LAO substrate. It is noted that the intergranular region present in the undoped film is absent in the Ag-doped film.

Furthermore, the energy dispersive x-ray analysis indicated that Ag was not detected in the Ag-doped film (HT4/4).

B. Films deposited at T_s = 400 °C

Figure 4 gives the low-magnification cross-sectional bright-field images of LSMO films with different doping levels of Ag and corresponding EDPs. A columnar grain structure is clearly observed in LT0/4 with an average width of 10 nm [Fig. 4(a)]. The columnar grains are basically perpendicular to the LSMO/LAO interface, and the size is relatively uniform. With increasing the Ag-doping level, the columnar structure was destroyed gradually. Especially for the film LT6/4 with the highest Ag-doping level, the columnar grains cannot be clearly resolved, and the growth direction is not completely perpendicular to the LSMO/LAO interface. Composite electron diffraction patterns of the cross-sectional samples were taken from areas including both the LSMO film and the LAO substrate. The slightly elongated diffraction spots along arcs [Figs. 4(b), 4(d), and 4(f)] suggest the decrease of epitaxial property in the LSMO films deposited at 400 °C in contrast to the high-quality epitaxy for those deposited at 750 °C. It is known that the substrate temperature had to be high enough (around T_s = 600 °C and above) to obtain good epitaxial growth using pulsed laser deposition (PLD).[24] Moreover, it is worthwhile to note the presence of additional diffraction spots for the Ag-doped films that are absent in the undoped ones, such as 111_{LSMO}, 111_{Ag}, and $\bar{2}02_{AgO}$ as indicated in Fig. 4(f).

Figures 5(a) and 5(b) show a plan-view bright-field image and the corresponding SAED pattern of the stoichiometric LSMO thin film (LT0/4). Typical granular grains are present in the film. The grain size is about 12 nm in diameter, significantly smaller than that of the undoped films deposited at 750 °C (50 nm). On the other hand, the diffraction spots of these plan-view samples elongated along arcs, indicating that the ab-plane alignment was also destroyed when the films were deposited at 400 °C.

Plan-view morphology and corresponding SAED patterns of Ag-doped films are shown in Figs. 5(c)–5(f). It can be seen that the most significant change in microstructure is that large clusters were formed in the doped films, with their amount and size increasing with Ag-doping. The average size of the large clusters in LT6/4 is around 60 nm in diameter. Moreover, in addition to the diffraction spots of $[001]_{LSMO}$ zone, diffraction spots of Ag, AgO, and other zones of LSMO were observed in Ag-doped films, such as 111_{LSMO}, 111_{Ag}, and 002_{AgO},

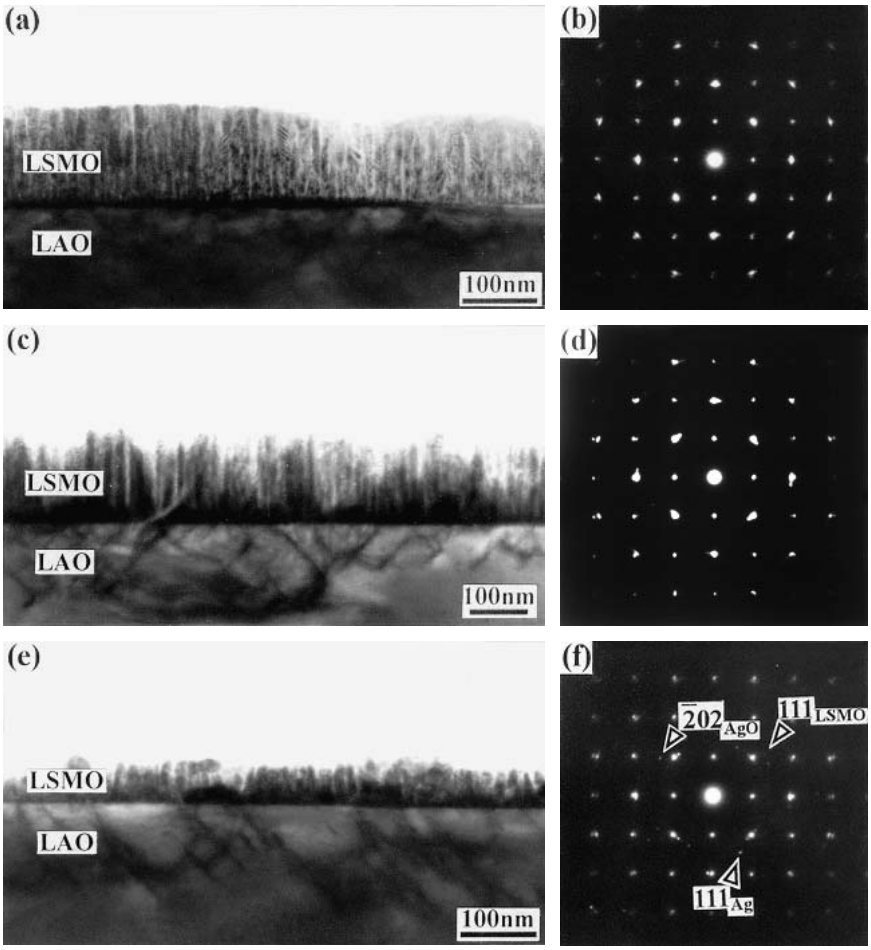

FIG. 4. Low-magnification cross-sectional bright-field images of the LSMO films deposited at 400 °C and the corresponding EDPs: (a,b) LT0/4, (c,d) LT3/4, (e,f) LT6/4.

as indicated in Fig. 5(f). This demonstrates the presence of elemental Ag and Ag oxide in the doped films. Meanwhile, the growth directions of some LSMO grains changed remarkably, giving additional diffraction spots of LSMO other than the $[001]_{LSMO}$ zone.

Besides the formation of large clusters in the Ag-doped films, the shape of normal LSMO grains became irregular, and the grain size increased gradually with Ag-doping. For LT6/4, the average grain size was around 20 nm and some grains coalesced [Fig. 5(e)].

The microstructure at atomic scale of these films was obtained by HREM observations. Figure 6(a) shows a plan-view HREM image of the undoped LSMO films. Some grains were connected, and low-angle grain boundaries were formed. The intergranular region also existed among the LSMO grains, similar to the undoped film deposited at 750 °C. For the doped LSMO films, some elemental Ag grains were found at the normal LSMO grain boundaries. Figure 6(b) shows such a Ag grain with its [110] direction perpendicular to the film surface. The size of the Ag grain is about 8 nm.

The high-magnification morphology of a large cluster in the Ag-doped film is shown in Fig. 7, as indicated by an arrow. Clearly, the large cluster consisted of several grains with irregular shape and different size. These grains have different orientations and do not exhibit typical granular morphologies. The polycrystalline clusters are mainly composed of LSMO and AgO grains. Figure 8(a) shows a HREM image of a large cluster with a AgO grain enclosed in LSMO grains. Elemental Ag grains can also be found at the LSMO grain boundaries, but less frequently, as shown in Fig. 8(b)

The composition analysis of the Ag-doped films was carried out by using EDS. Figure 9(a) shows a typical EDS spectrum of a large cluster. Ag peaks were clearly visible. Quantitative analysis showed that the content of Ag varied in different clusters, from several percent (i.e., 3 wt%) to tens of percent (i.e., 40 wt%). In contrast, no Ag has been detected in normal LSMO grains, as shown in Fig. 9(b). These compositional results, combined with the HREM results, demonstrate that Ag could not substitute into LSMO lattice but mainly

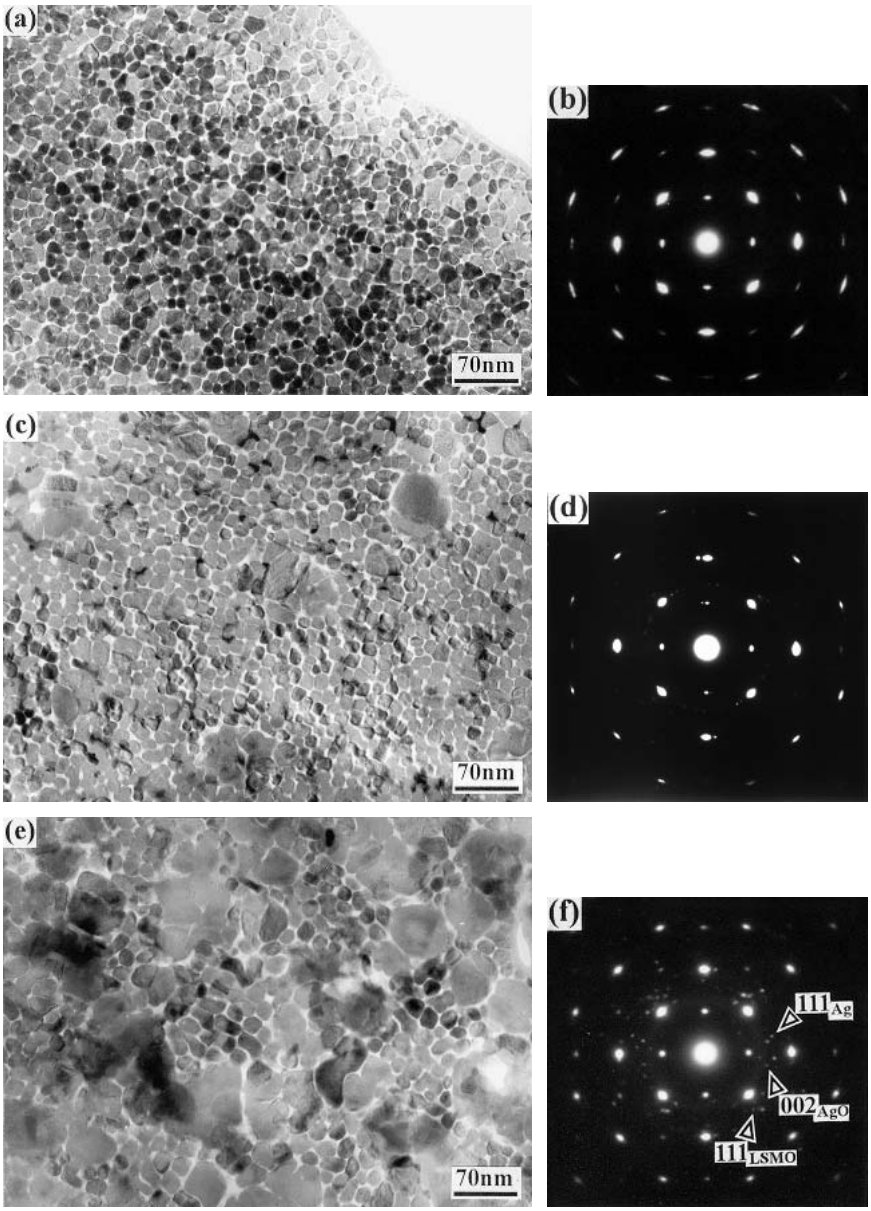

FIG. 5. Typical plan-view bright-field images of the LSMO films deposited at 400 °C and the corresponding EDPs: (a,b) LT0/4, (c,d) LT3/4, (e,f) LT6/4.

existed in the large polycrystalline clusters as AgO or at grain boundaries of normal LSMO grains in its elemental state.

IV. DISCUSSION

It has been shown that the effect of doping Ag on the microstructure of the LSMO films depends on the substrate temperature during deposition, and the effect is significant when the substrate temperature is low (i.e., 400 °C). A growth process for the LSMO-Ag system and properties of LSMO films with Ag doping are discussed in the following.

According to the data of room-temperature bond enthalpies, which give Ag–Ag as approximately 160 and Ag–O as approximately 220 mJ mol^{-1},[25] it is reasonable to conclude that Ag tends to oxidize in an oxygen ambient during PLD. Pinto *et al.* have also confirmed the fact, through optical spectroscopy, that AgO was indeed generated in the laser plum during PLD of Ag-doped $YBa_2Cu_3O_{7-\delta}$ films.[26] On the other hand, AgO is unstable at elevated temperatures (above 350 °C).[26]

When AgO arrives at a substrate surface at 750 °C, it dissociates into Ag and O again during *in situ* film formation. Not substituting into the LSMO lattice, At atoms diffuse to sites of lower free energy, typically grain

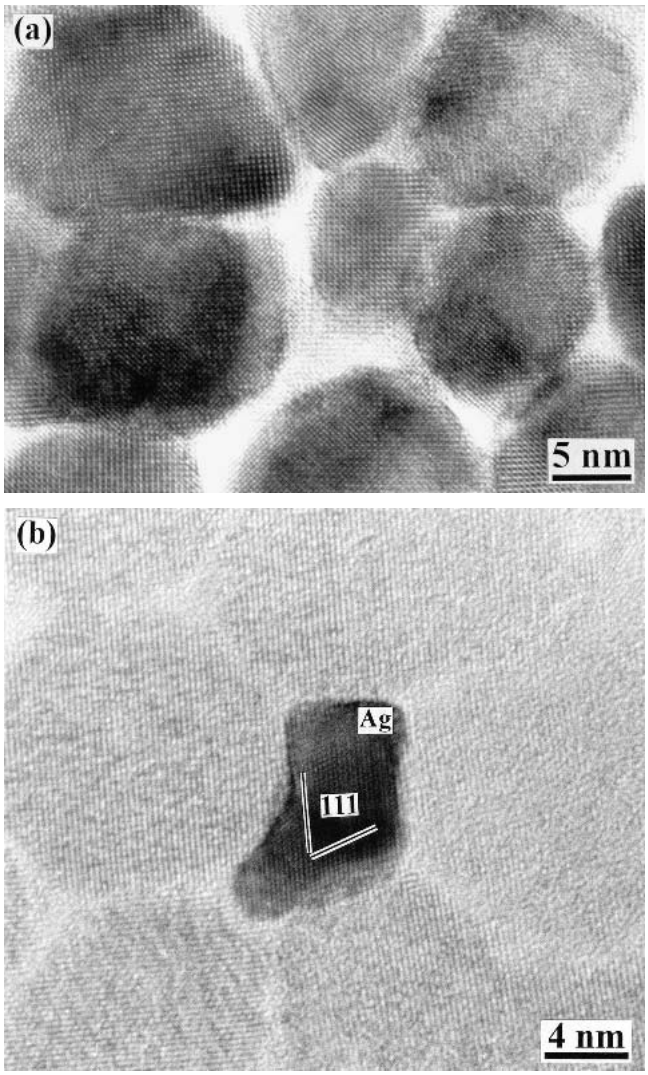

FIG. 6. Plan-view HREM images of the (a) undoped and (b) Ag-doped LSMO films deposited at 400 °C.

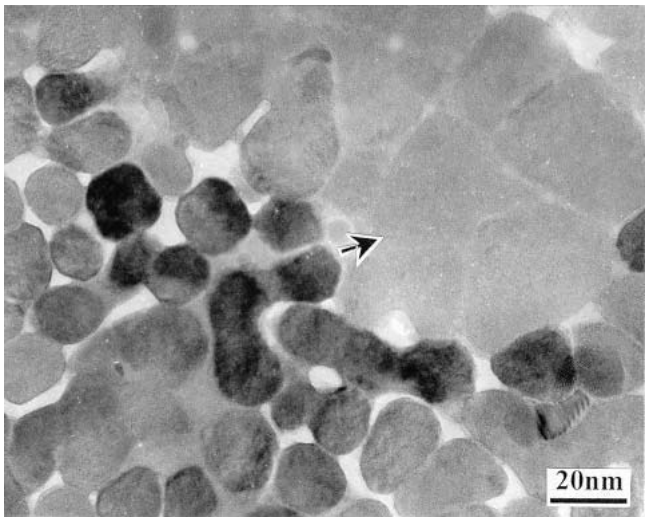

FIG. 7. High-magnification morphology of a large cluster consisting of several grains in the doped film.

boundaries, and segregate as agglomerates. During the diffusion, the Ag atoms impart their momentum to atoms of LSMO lattice, increasing the mobility of the latter. Such an effect is equivalent to an increase in annealing temperature. As a result, the Ag-doped films deposited at 750 °C are more perfect than the undoped films. The intergrain regions are eliminated by doping Ag. On the other hand, the saturated vapor pressure of Ag is fairly high at high temperatures, i.e., approximately 30 mtorr at 700 °C,[17] resulting in the re-evaporation of Ag atoms during the *in situ* annealing at 750 °C. Therefore, Ag could not be detected in the doped films deposited at 750 °C. This is in agreement with the previous report of x-ray diffraction and x-ray photoelectron spectroscopy results on Ag-doped LSMO films deposited at 750 °C.[27]

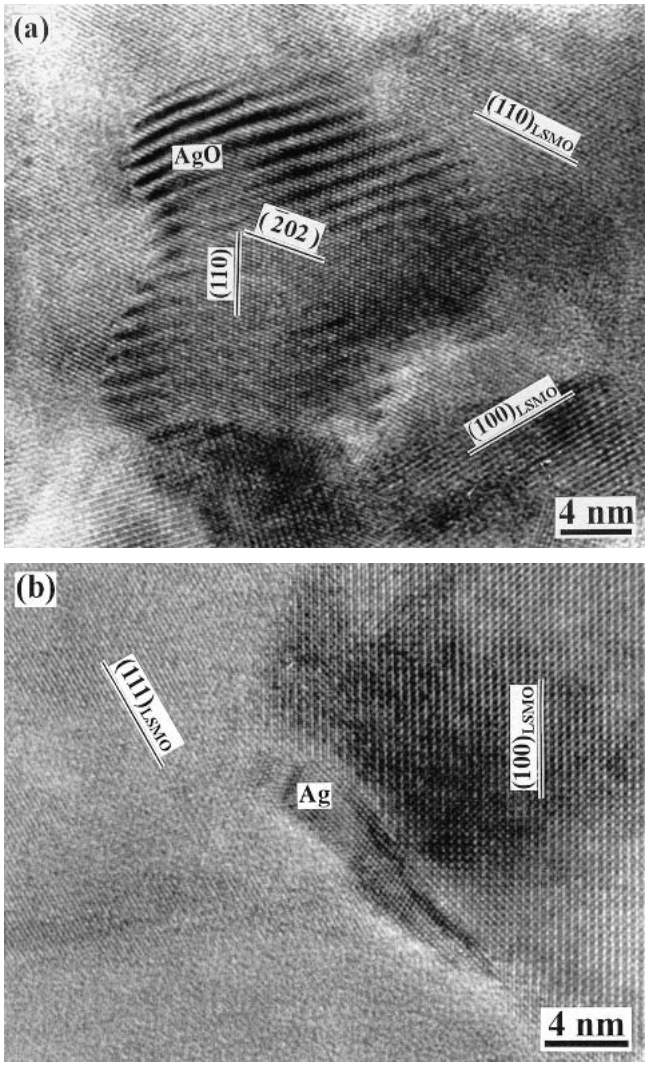

FIG. 8. HREM images of large clusters in the doped LSMO films. (a) AgO grain enclosed in LSMO grains. (b) Ag particle at the LSMO grain boundaries.

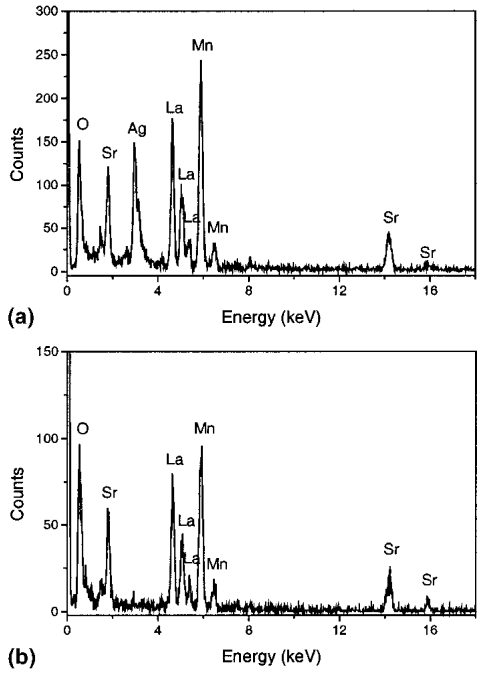

FIG. 9. (a) EDS of a large cluster in the doped film, where Ag peaks were clearly visible. (b) Nanometer-beam EDS analysis with a spatial resolution of 2–3 nm inside a LSMO grain, showing the absence of Ag.

When the substrate temperature was 400 °C, the decomposition of AgO deposited at the substrate surface could also occur. As discussed above, the decomposed Ag atoms agglomerated at the LSMO grain boundaries. At the same time, the diffusion of Ag atoms increased the mobility of atoms in LSMO grains, leading to the observed larger grain sizes. On the other hand, since the substrate temperature is not high enough, the decomposition of AgO could be incomplete, with some large AgO particles kept in the films. Due to the existence of these large AgO particles, the growth of the subsequent LSMO grains, especially those lay on the AgO particles, could not be epitaxial with respect to the LAO substrate. As a result, LSMO grains with different orientations were formed, giving the polycrystalline clusters.

The magnetotransport properties were measured at a low-field of 4 kOe for all of the films.[27] The MR values were similar for the doped and undoped LSMO films deposited at 750 °C, with a maximum of approximately 3% at the vicinity of T_c and declined with decreasing temperature. The MR values can even be ignored at 77 K. It is thus clear that the addition of Ag has no obvious effect on the magnetotransport properties of the epitaxial films deposited at 750 °C. This may be attributed to highly aligned grain boundaries in epitaxial films.

However, low-field MR of the Ag-doped LSMO films grown at $T_s = 400$ °C show a large enhancement compared to the undoped ones. In particular, the MR value at 77 K for doped films could be as large as 12% in a field of only 4 kOe, which is larger by a factor of two compared with the undoped one.[27] This large enhancement could be attributed to the existence of Ag and polycrystalline clusters in the doped films. The ferromagnetic spin alignment would show disordered status to some extent at the LSMO grain boundaries and AgO-LSMO interfaces in the polycrystallinelike clusters. Nonmagnetic metal Ag existing at the LSMO grain boundaries could also weaken the ferromagnetic interaction between grains and cause Mn spin disorder at the interfaces. They serve as a strong scatter centers for the highly spin-polarized conducting Mn^{3+} e_g electrons and lead to a high zero-field electrical resistance. Application of a moderate magnetic field can readily align the spin and drop the resistivity significantly. As a result, a large MR value at low magnetic field was obtained.

V. CONCLUSIONS

Cross-section and plan-view observations of changes in microstructure of LSMO films with different Ag-doping level were given in detail. The effect of doping Ag on the microstructure of the LSMO films depended on the substrate temperature during deposition, and the effect was significant when the substrate temperature was low (i.e., 400 °C). With decrease in the substrate temperature from 750 to 400 °C, epitaxial property of the LSMO films deteriorated. In the doped LSMO films deposited at 400 °C, large polycrystalline clusters consisting of LSMO, AgO, and Ag grains were formed, and Ag existed at the LSMO grain boundaries in its elemental state. This modified microstructure due to doping Ag could lead to an enhanced low-field MR value.

ACKNOWLEDGMENT

The authors gratefully acknowledge the support from the National Natural Science Foundation of China under Grant No. 50071063.

REFERENCES

1. J.M.D. Coey, J. Appl. Phys. **85,** 5576 (1999).
2. H.R. Khan, Mater. Sci. Forum **373–376,** 93 (2001).
3. C. Zener, Phys. Rev. **82,** 403 (1951).
4. H.Y. Hwang, S-W. Cheong, N.P. Ong, and B. Batlogg, Phys. Rev. Lett. **77,** 2041 (1996).
5. A. Gupta, G.Q. Gong, G. Xiao, P.R. Duncombe, P. Lecoeur, P. Trouilloud, Y.Y. Wang, V.P. Dravid, and J.Z. Sun, Phys. Rev. B **54,** 15629 (1996).
6. X.W. Li, A. Gupta, G. Xiao, and G.Q. Gong, Appl. Phys. Lett. **71,** 1124 (1997).
7. J.Y. Gu, C. Kwon, M.C. Robson, Z. Trajanovic, K. Ghosh, and R.P. Sharma, Appl. Phys. Lett. **70,** 1763 (1997).
8. H.L. Ju and H. Sohn, Solid State Commun. **102,** 463 (1997).
9. T. Walter, K. Dörr, K-H. Müller, B. Holzapfel, D. Eckert, M. Wolf, D. Schläfer, L. Schultz, and R. Grötzschel, Appl. Phys. Lett. **74,** 2218 (1999).

10. N.D. Mathur, G. Burnell, S.P. Isaac, T.J. Jackson, B-S. Teo, J.L. MacManus-Driscoll, L.F. Cohen, J.E. Evetts, and M.G. Blamire, Nature **387,** 266 (1997).
11. C. Kwon, Q.X. Jia, Y. Fan, M.F. Hundley, D.W. Reagor, J.Y. Coulter, and D.E. Peterson, Appl. Phys. Lett. **72,** 486 (1998).
12. C.J. Lu, Z.L. Wang, G.C. Xiong, and G.J. Lian, J. Mater. Res. **15,** 2454 (2000).
13. D. Kumar, M. Sharon, R. Pinto, P.R. Apte, S.P. Pai, S.C. Purandare, L.C. Gupta, and R. Vijayaraghavan, App. Phys. Lett. **62,** 3522 (1993).
14. A.Z. Moshfegh, Y.Q. Wang, Y.Y. Sun, A. Mesarwi, P.H. Hor, and A. Ignatiev, Physica C **218,** 396 (1993).
15. R. Pinto, P.R. Apte, S.P. Pai, and D. Kumar, Physica C **207,** 13 (1993).
16. D. Kumar, M. Sharon, P.R. Apte, R. Pinto, S.P. Pai, S.C. Purandare, C.P. D'Souza, L.C. Gupta, and R. Vijayaraghavan, J. Appl. Phys. **76,** 1349 (1994).
17. R. Kalyanaraman, S. Oktyabrsky, and J. Narayan, J. Appl. Phys. **85,** 6636 (1999).
18. R. Shreekala, M. Rajeswari, S.P. Pai, S.E. Lofland, V. Smolyaninova, K. Ghosh, S.B. Ogale, S.M. Bhagat, M.J. Downes, R.L. Greene, R. Ramesh, and T. Venkatesan, Appl. Phys. Lett. **74,** 2857 (1999).
19. T. Tao, Q.Q. Cao, K.M. Gu, H.Y. Xu, S.Y. Zhang, and Y.W. Du, Appl. Phys. Lett. **77,** 723 (2000).
20. R. Bathe, K.P. Adhi, S.I. Patil, G. Marest, B. Hannoyer, and S.B. Ogale, Appl. Phys. Lett. **76,** 2104 (2000).
21. C.K. Ong, S.Y. Xu, and W.Z. Zhou, Rev. Sci. Instrum. **69,** 3659 (1998).
22. Q. Zhan, R. Yu, L.L. He, D.X. Li, and X.N. Guo, Acta Metall. Sin. **37,** 337 (2001).
23. O.I. Lebedev, G. Van Tendeloo, S. Amelinckx, H.L. Ju, and K.M. Krishnan, Philos. Mag. A **80,** 673 (2000).
24. R. Von Helmot, J. Wecker, K. Samwer, L. Haupt, and K. Bärner, J. Appl. Phys. **76,** 6925 (1994).
25. J.A. Kerr, in *CRC Handbook of Chemistry and Physics 1999–2000,* edited by D.R. Lide (CRC Press, Boca Raton, FL, 1998).
26. R. Pinto, P.R. Apte, K.P. Adhi, S.B. Ogale, D. Kumar, and M.S. Hegde, J. Appl. Phys. **78,** 5204 (1995).
27. J. Li, Q. Huang, Z.W. Li, L.P. You, S.Y. Xu, and C.K. Ong, J. Phys.: Condens. Matter **13,** 3419 (2001).